

# The stellar content of the Hamburg/ESO survey<sup>★</sup>

## V. The metallicity distribution function of the Galactic halo

T. Schörck<sup>1</sup>, N. Christlieb<sup>2,3</sup>, J.G. Cohen<sup>4</sup>, T.C. Beers<sup>5</sup>, S. Shectman<sup>6</sup>, I. Thompson<sup>6</sup>, A. McWilliam<sup>6</sup>, M.S. Bessell<sup>7</sup>, J.E. Norris<sup>7</sup>, J. Meléndez<sup>8</sup>, S. Solange Ramírez<sup>9</sup>, D. Haynes<sup>10</sup>, P. Cass<sup>10</sup>, M. Hartley<sup>10</sup>, K. Russell<sup>10</sup>, F. Watson<sup>10</sup>, F.-J. Zickgraf<sup>1</sup>, B. Behnke<sup>11</sup>, C. Fechner<sup>12</sup>, B. Fuhrmeister<sup>1</sup>, P.S. Barklem<sup>3</sup>, B. Edvardsson<sup>3</sup>, A. Frebel<sup>13</sup>, L. Wisotzki<sup>14</sup>, and D. Reimers<sup>1</sup>

<sup>1</sup> Hamburger Sternwarte, Universität Hamburg, Gojenbergsweg 112, D-21029 Hamburg, Germany; e-mail: tschoerck/fzickgraf/dreimers@hs.uni-hamburg.de

<sup>2</sup> University of Heidelberg, Center for Astronomy, Landessternwarte, Königstuhl 12, D-69117 Heidelberg, Germany; e-mail: N.Christlieb@lsw.uni-heidelberg.de

<sup>3</sup> Department of Physics and Astronomy, Uppsala University, Box 515, SE-75120 Uppsala, Sweden; e-mail: barklem/be@fysast.uu.se

<sup>4</sup> Palomar Observatory, Mail Code 105-24, California Institute of Technology, Pasadena, CA 91125, USA; e-mail: jlc@astro.caltech.edu

<sup>5</sup> Department of Physics and Astronomy, CSCE: Center for the Study of Cosmic Evolution, and JINA: Joint Institute for Nuclear Astrophysics, Michigan State University, E. Lansing, MI 48824, USA; e-mail: beers@pa.msu.edu

<sup>6</sup> Carnegie Observatories of Washington, 813 Santa Barbara Street, Pasadena, CA 91101, USA; e-mail: shec/ian/andy@ociw.edu

<sup>7</sup> Research School of Astronomy and Astrophysics, Australian National University, Cotter Road, Weston, ACT 2611, Australia; e-mail: bessell/jen@mso.anu.edu.au

<sup>8</sup> Centro de Astrofísica da Univ. Porto, Rua das Estrelas, 4150-762 Porto, Portugal; e-mail: jorge@astro.up.pt

<sup>9</sup> IPAC, Mail Code 100-22, California Institute of Technology, Pasadena, CA 91125, USA; e-mail: solange@ipac.caltech.edu

<sup>10</sup> Anglo-Australian Observatory; PO Box 296, Epping, NSW 1710, Australia; e-mail: dmj/cpc/mh/ksr/fgw@aao.gov.au

<sup>11</sup> MPI for Gravitational Physics, Albert-Einstein-Institute, Am Mühlenberg, D-14476 Golm, Germany; e-mail: Berit.Behnke@aei.mpg.de

<sup>12</sup> Universität Potsdam, Institut für Physik und Astronomie, Karl-Liebknecht-Straße 24/25, D-14476 Potsdam, Germany; e-mail: cfech@astro.physik.uni-potsdam.de

<sup>13</sup> McDonald Observatory, The University of Texas at Austin, 1 University Station, C1400, Austin, TX 78712-0259; e-mail: anna@astro.as.utexas.edu

<sup>14</sup> Astrophysical Institute Potsdam, An der Sternwarte 16, D-14482 Potsdam, Germany; e-mail: lutz@aip.de

Received / Accepted

### Abstract.

We determine the metallicity distribution function (MDF) of the Galactic halo by means of a sample of 1638 metal-poor stars selected from the Hamburg/ESO objective-prism survey (HES). The sample was corrected for minor biases introduced by the strategy for spectroscopic follow-up observations of the metal-poor candidates, namely “best and brightest stars first”. Comparison of the metallicities  $[\text{Fe}/\text{H}]$  of the stars determined from moderate-resolution (i.e.,  $R \sim 2000$ ) follow-up spectra with results derived from abundance analyses based on high-resolution spectra (i.e.,  $R > 20,000$ ) shows that the  $[\text{Fe}/\text{H}]$  estimates used for the determination of the halo MDF are accurate to within 0.3 dex once highly C-rich stars are eliminated. We determined the selection function of the HES, which must be taken into account for a proper comparison between the HES MDF with MDFs of other stellar populations or those predicted by models of Galactic chemical evolution. The latter show a reasonable agreement with the overall shape of the HES MDF for  $[\text{Fe}/\text{H}] > -3.6$ , but none predict the sharp drop at  $[\text{Fe}/\text{H}] \sim -3.6$  present in the HES MDF. All theoretical MDFs, with the exception of the MDF predicted by the stochastic chemical enrichment model of Karlsson (2006), fail to represent the very sparse tail  $[\text{Fe}/\text{H}] < -4.0$  observed in the HES. A comparison with the MDF of Galactic globular clusters and of dSph satellites to the Galaxy shows good agreement with the halo MDF, derived from the HES, once the selection function of the latter is included.

**Key words.** stars: metal-poor - survey - galaxy: evolution - halo

## 1. Introduction

One of the key observables for constraining models of the formation and chemical evolution of the Galaxy is the Metallicity Distribution Function (MDF) of the constituent stars of its various components (bulge, disk, halo). The MDF provides critical information on the enrichment history of those components with heavy elements. In the case of the halo, early enrichment may have been provided by the very first generations of massive stars, formed from material of primordial composition shortly after the Big Bang (i.e., Population III stars).

Models of Galactic chemical evolution need to be compared to an accurate (and precise) observed halo MDF to test their predictions, to constrain their various parameters (such as the effective yield, the star-formation rate and the IMF), and in order to obtain information on the properties of Population III stars that are responsible for the earliest enrichment. This is particularly important for the lowest metallicity tail of the MDF, which provides invaluable information on the earliest enrichment phases (Prantzos 2003); for instance, it has been suggested that a minimal metallicity value (around  $10^{-4}$  solar for Fe, or  $\sim 10^{-3.5}$  for O) is required to form low-mass stars (Bromm & Loeb 2003; Frebel et al. 2007; see also, e.g., Omukai 2000; Bromm et al. 2001; Umeda & Nomoto 2003).

The accuracy of a derived halo MDF increases directly with the total number of observed metal-poor halo stars. Selection of such stars without the introduction of a kinematic bias (e.g., from among high proper motion stars) makes them of particular utility for examination of the relationships between the chemistry and kinematics of the halo. Early determinations of the halo MDF were based on small samples of globular clusters (Hartwick 1976;  $N = 60$ ), or a mixture of halo subdwarfs and globular clusters (Bond 1981;  $N = 90$  and  $N = 31$ , respectively). Problems with these samples arise not only from their small sizes, but also their inaccurate metallicities. Later studies employed significantly larger samples with spectroscopically-determined stellar abundances. For example, Ryan & Norris (1991) used a sample of 372 kinematically-selected halo stars. Ryan & Norris (1991) and Carney et al. (1996) showed that the MDF peaks at a metallicity of  $[\text{Fe}/\text{H}] = -1.6$  with wings from  $[\text{Fe}/\text{H}] = -3.0$  to solar abundances.

The HK-survey (Beers et al. 1985, 1992; Beers 1999), originated by Preston and Shtetman, and greatly extended by Beers to include several hundred additional objective-prism plates, was (until the advent of the HES) the primary source of metal-poor candidates suitable for consideration of the halo MDF. With the assistance of numerous colleagues, medium-resolution spectroscopy of over 10,000 HK-survey stars was obtained, using 1.5 m–4 m class telescopes, over the past two decades. This led to the identification of thousands of stars with  $[\text{Fe}/\text{H}] < -2.0$ , as well as significant numbers of stars with  $[\text{Fe}/\text{H}] < -3.0$ . It is perhaps of interest that the HK survey

has not (to date) yielded any stars with  $[\text{Fe}/\text{H}] < -4.0$  confirmed by high-resolution spectroscopy; this may be related to the fact that the HK survey reaches apparent magnitudes that are brighter than the HES, and as a result is dominated more than the HES by inner-halo stars.

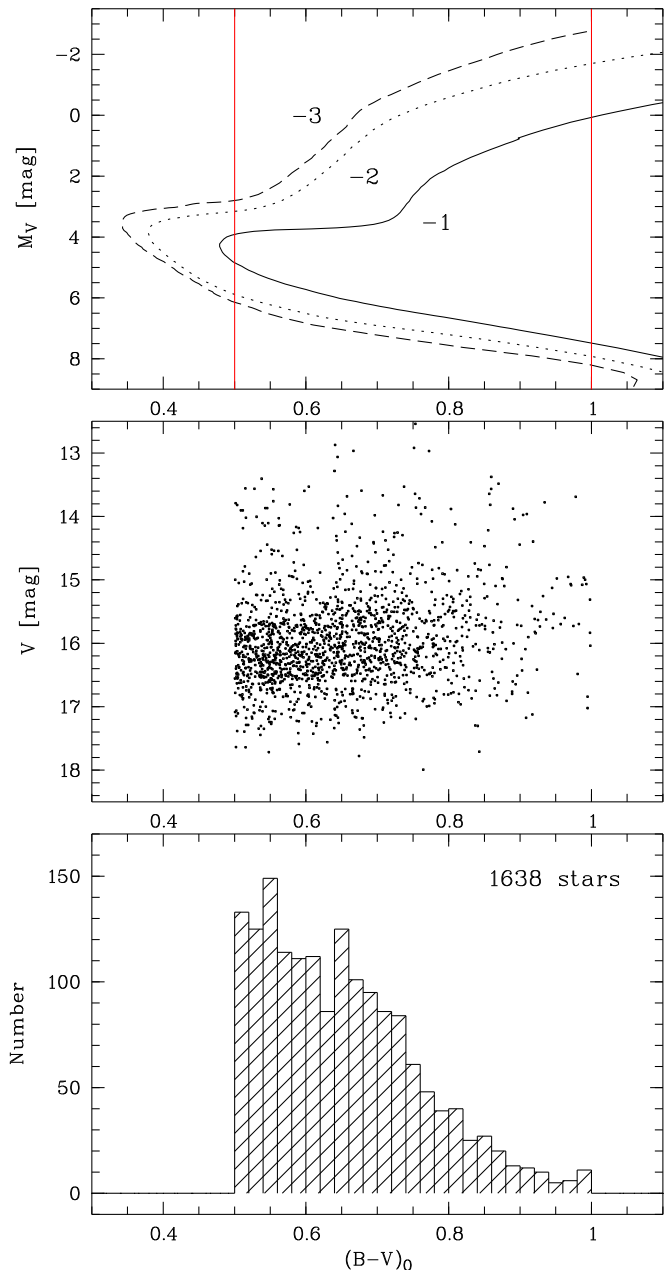


**Fig. 1.** Upper panel: Isochrones for an age of 12 Gyr and metallicities of  $[\text{Fe}/\text{H}] = -1$ ,  $-2$ , and  $-3$  (Kim et al. 2002), and chosen colour cuts (see text for details); middle panel:  $V$  magnitude distribution of the HES sample from which we construct the halo MDF; lower panel:  $(B - V)_0$  distribution.

Send offprint requests to: N. Christlieb,  
e-mail: N.Christlieb@lsw.uni-heidelberg.de

\* Based on observations collected at Las Campanas Observatory, Palomar Observatory, Siding Spring Observatory, and the European Southern Observatory (Proposal IDs 69.D-0130, 170.D-0010, 073.D-0555, and 081.D-0596).

The Sloan Digital Sky Survey (SDSS; Gunn et al. 1998, York et al. 2000), and in particular the Sloan Extension for Galactic Understanding and Exploration (SEGUE), has provided even larger samples of halo stars, as discussed by

Carollo et al. (2007) and by Ivezić et al. (2008). The former emphasize the division of the halo into two structural components, an inner region with  $R < 10\text{--}15$  kpc, and an outer region beyond that radius. These two components differ in stellar metallicities, stellar orbits, and spatial density profiles. As we discuss in Sect. 2 below, the HES sample is dominated by inner-halo stars. We note that we hereafter refer to the inner halo as “the halo”, unless indicated otherwise.

In spite of the very large sample of  $\sim 20,000$  stars used by Carollo et al., their coverage of the regime of very low metallicity is limited. According to their supplemental Fig. 4, they find only 3 stars with  $[\text{Fe}/\text{H}] < -3.0$  in their “local sample” of 10,123 stars. The main reason for this is that the stars of their sample were not selected to be metal-poor, but for the purpose of spectrophotometric and telluric calibration of the SDSS spectra.

Recent high-resolution spectroscopic followup of stars from the Carollo et al. sample (W. Aoki, priv. comm.) has indicated that the current version of the SEGUE Stellar Parameter Pipeline (SSPP; see Lee et al. 2008b,a; Prieto et al. 2008) is somewhat conservative in the assignment of stellar metallicity estimates, in the sense that stars assigned  $[\text{Fe}/\text{H}] < -2.7$  by the SSPP are in reality more metal-deficient, on average, by on the order of 0.3 dex. A recent examination of the numbers of stars from the SDSS/SEGUE survey, taking into account this offset, suggests that up to several hundred stars with  $[\text{Fe}/\text{H}] < -3.0$  are in fact present in the current SDSS sample of stars (including other categories of targets than just the calibration stars).

Ivezić et al. (2008) focus on the comparison between the inner halo and the disk. Since they rely on abundances determined from photometry, they cannot reliably determine Fe-metallicities of stars at  $[\text{Fe}/\text{H}] < -2$ . Nevertheless, the metallicity map of some 2.5 million stars with photometric metallicities shown in Fig. 8 of Ivezić et al. indicates that there exist very large numbers of stars in SDSS consistent with  $[\text{Fe}/\text{H}] < -2.0$ . Follow-up spectroscopy is, at present, only available for a subset of them. Beers et al. (in preparation) discuss the MDF of the lowest metallicity stars found in SDSS/SEGUE. The total number of stars with  $[\text{Fe}/\text{H}] < -2.0$ , based on medium-resolution SDSS spectroscopy, is over 15,000 (i.e., triple the number discovered by the combination of the HK and HES).

Another wide-angle spectroscopic survey is the Hamburg/ESO objective-prism survey (HES). It was originally conceived as a survey for bright quasars (Reimers 1990; Wisotzki et al. 1996, 2000); however, its data quality is sufficient to not only efficiently select quasars with redshifts of up to  $z = 3.2$ , but also various types of stellar objects. In this paper we are mainly concerned with the low-metallicity tail of the halo MDF, which is constructed from a sample of 1638 metal-poor stars selected in the HES by quantitative criteria. This paper continues our series on the stellar content of the HES (Christlieb et al. 2001b, Paper I; Christlieb et al. 2001a, Paper II; Christlieb et al. 2005, Paper III; Christlieb et al. 2008b, Paper IV).

The compilation of the sample of metal-poor stars is described in Sect. 2; the follow-up observations and determination of the metallicities are described in Sect. 3. In Sect. 4 we detail how the MDF was constructed. Comparisons of the

observed MDF with MDFs predicted by models of Galactic chemical evolution are presented in Sect. 5, and a comparison with the MDFs of the Galactic globular cluster system and dwarf spheroidal galaxies is presented in Sect. 6. The results are discussed in Sect. 7.

**Table 1.** Number of stars in each candidate class in the total sample of candidates, number of observed candidates, and number of accepted candidates after removal of emission line objects, “peculiar” objects (e.g., objects with continuous spectra) and all stars with a G-band index  $\text{GP} > 6 \text{ \AA}$ . In the last column, we list the scaling factors applied to the  $[\text{Fe}/\text{H}]$  histograms for each candidate class during the construction of the MDF (see Section 4).

Class	Number of stars			Factor
	All	Observed	Accepted	
mpca	201	123	105	1.63
unid	231	208	192	1.11
mpcb	2006	1008	940	1.99
mpcc	1275	432	401	2.95
Sum	3713	1771	1638	

## 2. The metal-poor star sample

One of the main advantages of the HES for determining the halo MDF is that the selection of candidate metal-poor stars was done with quantitative criteria. Hence, the selection is well-understood, and possible selection biases can be quantified and corrected for during the construction of the MDF. Furthermore, the selection is purely spectroscopic, so it does not introduce any kinematic biases.

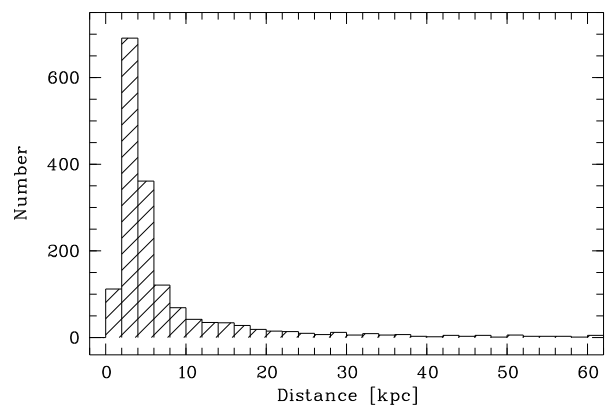


**Fig. 2.** Distance distribution of the HES sample. The sample is dominated by stars at distances of less than  $\sim 5$  kpc from the Sun; a few cool giants are located at distances of up to  $\sim 50$  kpc.

The selection of candidates in the HES is described in Paper IV. For the sample used in this study, we employed only the  $\text{KP}/(B - V)_0$  selection; i.e., a star is selected as a metal-poor candidate if its KP index of the Ca II K line, as measured

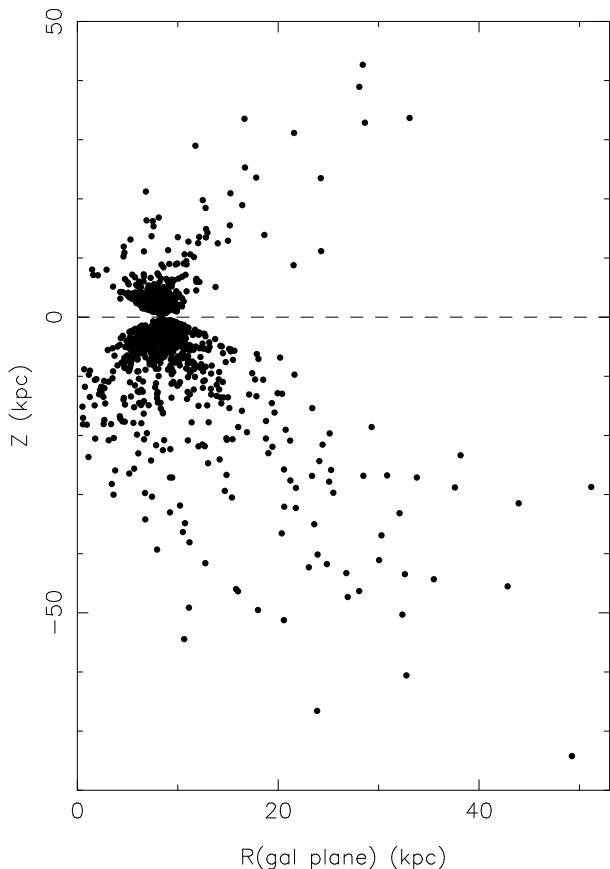


**Fig. 3.** Spatial distribution of the HES sample.  $R(\text{gal. plane})$  is the distance from the Galactic center projected onto the Galactic plane.

in its digital HES objective-prism spectrum, is smaller than the KP index predicted for a star of  $[\text{Fe}/\text{H}] = -2.5$  and the same  $(B - V)_0$  colour (see Fig. 4 of Paper IV). This cutoff was chosen because it results in a good compromise between completeness at  $[\text{Fe}/\text{H}] < -3.0$ , the region in  $[\text{Fe}/\text{H}]$  we are mainly interested in because it corresponds to the earliest phases of Galactic chemical evolution, and achieving a selection which efficiently rejects stars at higher metallicity. In addition to the KP index, the  $B - V$  colours are measured in the HES spectra as well (see Paper IV for details), and then are corrected for reddening using the maps of Schlegel et al. (1998). We restrict the sample to the colour range  $0.5 < (B - V)_0 < 1.0$ , because the follow-up observations of stars bluer than  $(B - V)_0 = 0.5$  have not yet reached a sufficient level of completeness, and for stars redder than  $(B - V)_0 = 1.0$ , the accuracy of the determination of  $[\text{Fe}/\text{H}]$  from moderate-resolution follow-up spectra is limited due to the lack of calibration stars and the weakness of the  $\text{H}\delta$  line, which is used as a temperature indicator. The  $V$  magnitude and  $(B - V)_0$  distribution of our sample together with isochrones for an age of 12 Gyr and different metallicities is shown in Fig. 1. The  $V$  magnitudes are from the HES.

The selection was applied to all spectra of unsaturated point sources extracted on 329 (out of 379) HES plates, covering a nominal area of  $\sim 7700 \text{ deg}^2$  of the southern high galactic latitude sky. The candidates were visually inspected and assigned

to the classes *mpca*, *unid*, *mpcb*, and *mpcc*. As described in Paper IV, the classification is based on the appearance of the  $\text{Ca II K}$  line in the digital HES spectra. Candidates of class *mpca* are the best in terms of the success rate of finding stars at  $[\text{Fe}/\text{H}] < -2.5$  (see Fig. 7), since no  $\text{Ca II K}$  line could be seen in the HES spectrum, while the candidates of class *mpcc* are the worst, because a strong  $\text{Ca K}$  line could clearly be seen. However, the  $\text{Ca K}$  line is still strong in cool, moderately metal-poor (i.e.,  $[\text{Fe}/\text{H}] \sim -2.0$ ) giants, therefore the line is expected to be detected in the HES spectra of such stars. For statistical studies such as the determination of the halo MDF it is therefore necessary to obtain follow-up spectroscopy also of the *mpcc* candidates, because otherwise a color-related bias would be introduced. Furthermore, the assignment of the classes to the candidates is subjective, and therefore it would be impossible to determine the selection function of the HES if only a subset of the candidates selected by quantitative criteria would be considered for the construction of the MDF.

The result of the visual inspection are 3792 accepted candidates, of which 79 are present on multiple plate quarters or plates; the number of unique candidates is 3713. The number of candidates in each of the aforementioned classes is listed in Tab. 1. Only about half of the 3713 candidates are part of the sample presented in Tab. A.1 of Paper IV. This is because slightly improved sky background and spectrum extraction algorithms were used in the final reduction of the HES, from which the sample of Paper IV was drawn. Note that minor changes of the reduction algorithms can have a large effect on the measurement of the KP index, because the  $\text{Ca II K}$  line is covered by only four pixels of the HES spectra.

We determine distances to each of the sample stars using the  $[\text{Fe}/\text{H}]$  for each star and a set of isochrones similar to those shown in the upper panel of Fig. 1. Assuming that all the sample stars are at or above the main sequence turnoff, we obtain the distance distribution shown in Fig. 2, and the spatial distribution shown in Fig. 3. The cooler giants in our sample reach distances from the Galactic plane well beyond  $|Z| = 15 \text{ kpc}$ . However, the sample is clearly dominated by inner halo stars. There is a hint that the outer halo stars with  $|Z| > 15 \text{ kpc}$  have a higher fraction of extremely metal-poor stars than do those of the inner halo with  $5 < |Z| < 15 \text{ kpc}$ , but given the wide range in metallicity we see throughout the halo, our sample is too small to determine the MDFs of the inner and outer halo separately with confidence.

### 3. Determination of metallicities

For 1771 of the 3713 unique candidates, moderate-resolution spectroscopy was obtained with various telescope/instrument combinations (see Tab. 2). The candidates were mostly observed in programs aiming at the identification of targets for high-resolution spectroscopy of the most metal-poor stars. Hence, the observing strategy adopted for the follow-up observations was to observe the brightest and best candidates (i.e., candidate classes *mpca* and *unid*) first.

In the follow-up spectra, we measured the KP index as well as the HP2 index of  $\text{H}\delta$  and the GP index for the G-band of CH (see Beers et al. 1999 for the definition of these indices). When

**Table 2.** Follow-up observations of the candidate metal-poor stars.

Telescope(s)	Instrument(s)	Observers	$N_{\text{stars}}$
Magellan 1&2	B&C	Shectman, McWilliam, Thompson	553
SSO 2.3 m	DBS	Bessell, Norris, Edvardsson, Behnke, Christlieb, Frebel	339
Palomar 200"	DS	Cohen, Ramírez, Melendez	323
UK Schmidt	6dF	Haynes, Cass, Hartley, Russell, Watson	283
ESO 3.6 m	EFOOSC2	Fechner, Zickgraf, Barklem, Fuhrmeister, Christlieb	140
Total			1638

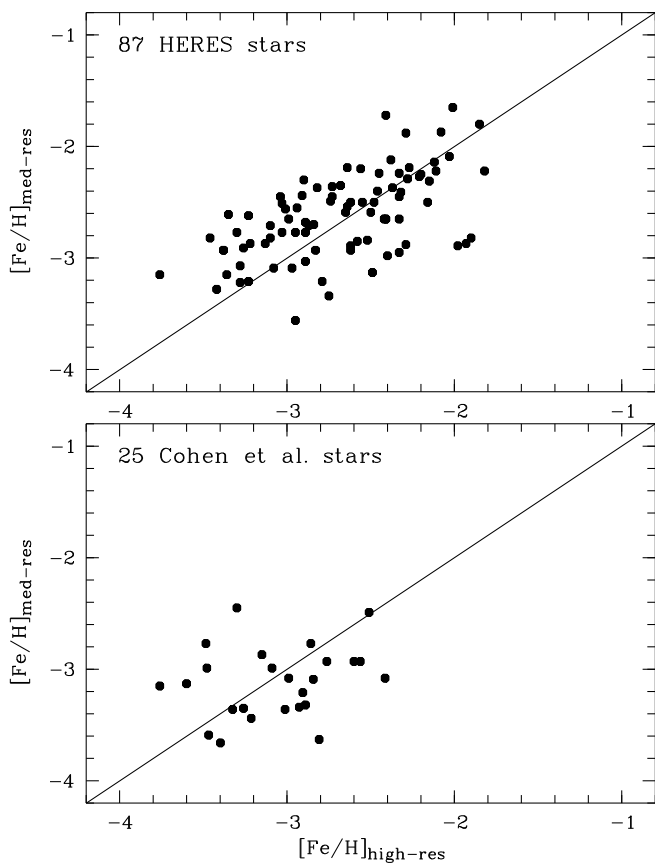


**Fig. 4.** Comparison of determinations of  $[\text{Fe}/\text{H}]$  from moderate-resolution follow-up spectra with results based on high-resolution spectroscopy. Upper panel: 87 stars observed with VLT/UVES (Barklem et al. 2005). Lower panel: 23 stars observed with Keck/HIRES and two with Magellan/MIKE; analyses carried out by Cohen et al. (2004), Cohen et al. (2006), Cohen et al. (2008), and Cohen (2008, unpublished).

multiple spectra for a star were available, the  $S/N$ -weighted average of the individual line index measurements was adopted.  $[\text{Fe}/\text{H}]$  was determined from the adopted HP2 and KP indices using an updated version of the method of Beers et al. (1999).

Since the stars of our sample were observed with many telescope/instrument combinations, it is important to verify that there are no systematic offsets between the measurements of the line indices in spectra taken at different telescopes. Such

offsets could occur, for example, if the CCD response curves would strongly vary from instrument to instrument in the wavelength ranges in which the line and continuum bands of the indices are measured. For this reason, a number of candidate metal-poor stars were intentionally re-observed at different telescopes. Furthermore, in most of the observing campaigns, spectra of a few metal-poor standards (e.g., G 64–12, HD 140283, or CD  $-38^\circ$  245) as well as metal-poor radial velocity standards were secured. In Fig. 5, we show comparisons of the KP and HP2 indices measured in spectra taken with all relevant telescope/instrument combinations. In total, 315 pairs of measurements are available. No systematic offsets between the measurements can be seen. However, the scatter of the measurements in spectra obtained with the UK Schmidt and the fibre-fed multi-object spectrograph 6dF are about a factor two larger than those of the other telescope/instrument combinations. This can be attributed to the fact that sky subtraction is more difficult for the 6dF spectra, since only a few fibers were dedicated to measure the sky background, and furthermore the sky brightness might have varied over the  $6^\circ$  diameter field of view of the instrument.

The quality of the spectra (i.e.,  $R \sim 2000$  and a typical  $S/N$  of 20 per pixel in the continuum near the Ca K line) allowed the easy identification and rejection of emission-line and other “peculiar” objects (e.g., galaxies, or objects with continuous spectra, such as cool helium-rich white dwarfs). It has been shown by Cohen et al. (2005) that CH lines present in the continuum bands of the KP and HP2 indices lead to a systematic underestimation of these indices, resulting in systematically too low  $[\text{Fe}/\text{H}]$  values. Hence, we also excluded from this study all stars with  $\text{GP} > 6 \text{ \AA}$ . Since the fraction of carbon-enhanced stars among metal-poor stars increases as the metallicity decreases (see, e.g., Cohen et al. 2005; Lucatello et al. 2006), the rejection of stars with strong G-bands might lead to a bias against low-metallicity stars. However, since only 90 stars, or 5% of the 1771 observed stars, were rejected due to this reason, the effect on our sample is only minor. We also note that the three currently-known ultra metal-poor stars (i.e., stars with  $[\text{Fe}/\text{H}] < -4.0$ ; see Sect. 4 below), all of which have large overabundances of carbon, are not rejected by this criterion, since their GP indices are smaller than  $6 \text{ \AA}$ . In total, 133 stars were rejected, leaving 1638.

Homogeneous abundance analyses based on high-resolution spectra are available for 112 of the confirmed candidates in our sample. The spectra were taken with VLT/UVES

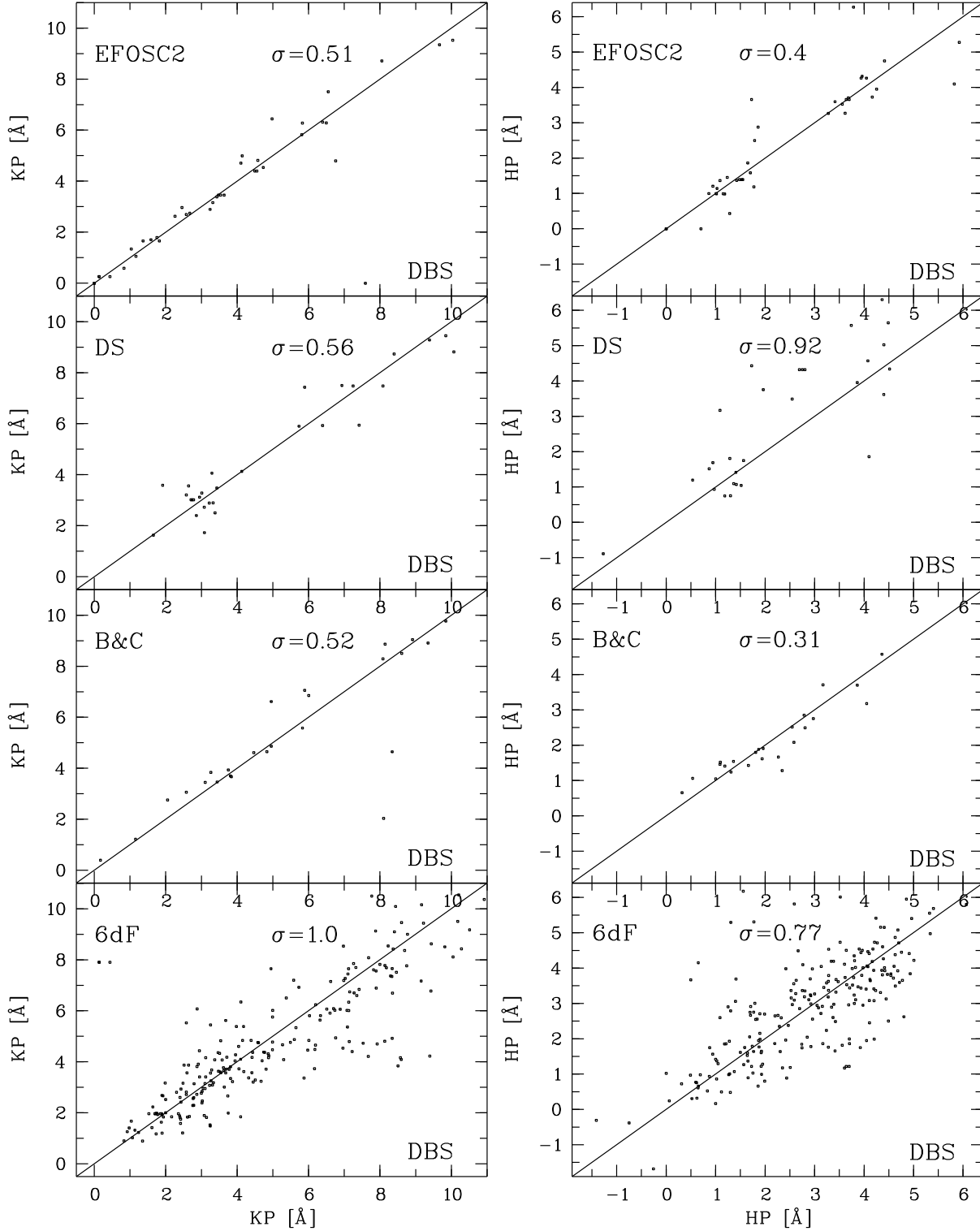


**Fig. 5.** Pairs of KP and HP2 measurements for the same star in spectra obtained with different telescope/instrument combinations. Note that some of the estimates of  $\sigma$  displayed in the panels are influenced by a number of outliers; i.e., robust estimates would yield smaller values.

(87 stars), Keck/HIRES (23 stars) or Magellan/MIKE (2 stars). The abundance analyses were performed by Barklem et al. (2005), Cohen et al. (2004), Cohen et al. (2006), Cohen et al. (2008), and Cohen (2007, unpublished). Fig. 4 compares the

iron abundances determined in the course of these analyses ( $[\text{Fe}/\text{H}]_{\text{high-res}}$ ) to the moderate-resolution follow-up results ( $[\text{Fe}/\text{H}]_{\text{med-res}}$ ). No significant trends or offsets are present, and the  $1\text{-}\sigma$  scatter around a regression line of the combined

test sample is 0.3 dex. We hence conclude that the accuracy of  $[\text{Fe}/\text{H}]_{\text{med-res}}$  for our sample is  $\pm 0.3$  dex. We note that the accuracy can be increased especially for the cooler stars by using CCD photometry rather than  $B - V$  colors predicted from the  $\text{H}\delta$  index HP2 when deriving  $[\text{Fe}/\text{H}]_{\text{med-res}}$ . However, CCD photometry is not yet available for all stars of our sample.

To increase the accuracy of the determination of the shape of the low-metallicity tail of the MDF, we replaced  $[\text{Fe}/\text{H}]_{\text{med-res}}$  with  $[\text{Fe}/\text{H}]_{\text{high-res}}$ , where available.  $[\text{Fe}/\text{H}]_{\text{high-res}}$  values are available for 27 of the 76 stars at  $[\text{Fe}/\text{H}]_{\text{med-res}} < -3.0$ , and five out of the six with  $[\text{Fe}/\text{H}]_{\text{med-res}} < -3.5$ . The  $[\text{Fe}/\text{H}]_{\text{high-res}}$  values were taken from the above mentioned references and from Cayrel et al. (2004) for HE 0305–5442, a re-discovery of CS 22968-014 ( $[\text{Fe}/\text{H}]_{\text{high-res}} = -3.56$ ). The sixth star at  $[\text{Fe}/\text{H}]_{\text{med-res}} < -3.5$  in our sample for which a  $[\text{Fe}/\text{H}]_{\text{high-res}}$  estimate is available has  $[\text{Fe}/\text{H}]_{\text{med-res}} = -4.2$ . A VLT/UVES spectrum exists for this star, and a preliminary abundance analysis confirms that the star has a metallicity close to or slightly below  $[\text{Fe}/\text{H}] = -4.0$ . Due to the preliminary nature of this result, we do not show this data point in Fig. 4.

#### 4. Construction of the observed MDF

In order to investigate potential selection biases given the adopted follow-up observation strategy, it is instructive to compare the MDFs derived from stars of the individual candidate classes and in different magnitude ranges. For the purpose of investigating the possible presence of a bias caused by the fact that the brightest stars were observed first, we divided the HES sample into a bright ( $B \leq 16.7$  mag) and a faint ( $B > 16.7$  mag) half. In Fig. 6, one can see that the shapes of the MDFs of each of the four candidate classes, as well as those of the total sample, do not differ significantly from each other.

We then divided the sample according to candidate class and compared the MDFs of these subsamples. As can be seen in Fig. 7, the fraction of stars at  $[\text{Fe}/\text{H}] < -3.0$  is highest among the mpca candidates (i.e., 7%), and significantly lower in the other classes (i.e., 3–4%). That is, the MDF of mpca candidates is biased towards lower metallicities. Fig. 7 also shows that the number of false positives (i.e., stars at  $[\text{Fe}/\text{H}] > -2.5$ ) is considerably higher among the mpcc candidates. However, this contamination does not affect our study significantly, because we are mainly concerned with the low-metallicity tail of the MDF.

In order to properly take into account the stars of our candidate sample for which no spectroscopic follow-up observations exist, we constructed MDFs from the observed sample of stars in the following two ways. First, we computed separate MDFs for each of the candidate classes and scaled them such that the correct relative fraction of stars is produced when the four scaled MDFs are coadded; i.e., the scaling factors listed in the last column of Tab. 1 were applied. Secondly, we assigned to each of the 1942 stars in the full candidate sample lacking follow-up observations the  $[\text{Fe}/\text{H}]$  of a randomly selected star of the same candidate class for which a follow-up spectrum is available. We also randomly rejected stars with a too strong G-band and “peculiar” stars according to the probabilities deter-

mined from the sample for which follow-up observations exist. In this way, a sample of 3439 stars with the correct relative fraction of the candidates of the four classes is created.

The MDFs produced by these two methods are expected to be very similar to each other, because in each of them, the class-wise MDFs are scaled and then added to produce the final MDF; only the scaling methods are slightly different. Indeed, as can be seen in Fig. 8, the results do not differ significantly from each other. We adopt the MDF constructed by means of scaling the class-wise MDFs by a factor and adding them up. For this MDF, the numbers of stars in each metallicity bin are listed in Tab. 3.

A prominent feature in both of the scaled MDFs is a sharp drop at  $[\text{Fe}/\text{H}] \sim -3.6$  (see Fig. 8); in our (scaled) sample, only two out of 3439 stars have  $[\text{Fe}/\text{H}] < -3.6$ . Such a drop was also recognized by Norris (1999), and it has been seen in the Hamburg/ESO R-process Enhanced star Survey (HERES; see Fig. 2 of Barklem et al. 2005). It reflects the fact that only very few stars at  $[\text{Fe}/\text{H}] < -3.6$  were found in projects aiming at the identification and detailed study of the lowest metallicity stars of the Galactic halo, despite of considerable effort being expended to find them (see, e.g., Cohen et al. 2008 and references therein).

The shape of the low-metallicity end of the halo MDF could not be determined accurately by Ryan & Norris (1991) due the limited size of their sample, which contains only four stars at  $[\text{Fe}/\text{H}] < -3.4$ , and none with  $[\text{Fe}/\text{H}] < -4.0$ . As can be seen in Fig. 9, in the range  $-3.4 < [\text{Fe}/\text{H}] < -2.5$  their halo MDF agrees extremely well with ours when their MDF is corrected for the selection used in the HES. In Fig. 9 one can see a disagreement between the two MDFs in the bin centered on  $[\text{Fe}/\text{H}] = -3.5$ . However, due to the small number of stars in the sample of Ryan & Norris at this metallicity, the difference is not significant.

Another feature of the halo MDF is a lightly populated tail extending to  $[\text{Fe}/\text{H}] < -5.0$ . The evidence for this feature from our (scaled) sample alone is weak, since it contains only two stars at  $[\text{Fe}/\text{H}] < -3.6$ , and none at  $[\text{Fe}/\text{H}] < -4.3$ . However, currently some 10 stars with  $[\text{Fe}/\text{H}] < -3.6$  have published abundance analysis based on high-resolution spectroscopy (see Tab. 4 of Beers & Christlieb 2005 for a recent review), including three additional stars at  $[\text{Fe}/\text{H}] < -4.0$ : HE 1327–2326 ( $[\text{Fe}/\text{H}] = -5.4$ ; Frebel et al. 2005; Aoki et al. 2006; Frebel et al. 2006a), HE 0107–5240 ( $[\text{Fe}/\text{H}] = -5.7$ ; Christlieb et al. 2002, 2004; Bessell et al. 2004; Christlieb et al. 2008a), and HE 0557–4840 ( $[\text{Fe}/\text{H}] = -4.8$ ; Norris et al. 2007). These three stars are not part of our sample due to a variety of reasons. HE 1327–2326 is part of the bright HES metal-poor sample consisting of stars above a saturation threshold (Frebel et al. 2006b), while only unsaturated point sources entered the sample of this work. HE 0107–5240 was selected in a previous version of the candidate selection which was slightly less restrictive than the one we use here; as a result, this star misses the selection cutoff of 3.9 Å for its HES ( $B - V$ )<sub>0</sub> colour of 0.6 mag by 0.1 Å (the KP index measured in the HES spectrum is 4.0 Å). And finally, HE 0557–4840 is located on one of the 50 HES plates which are not considered here. In conclusion, for an accurate determination of the shape

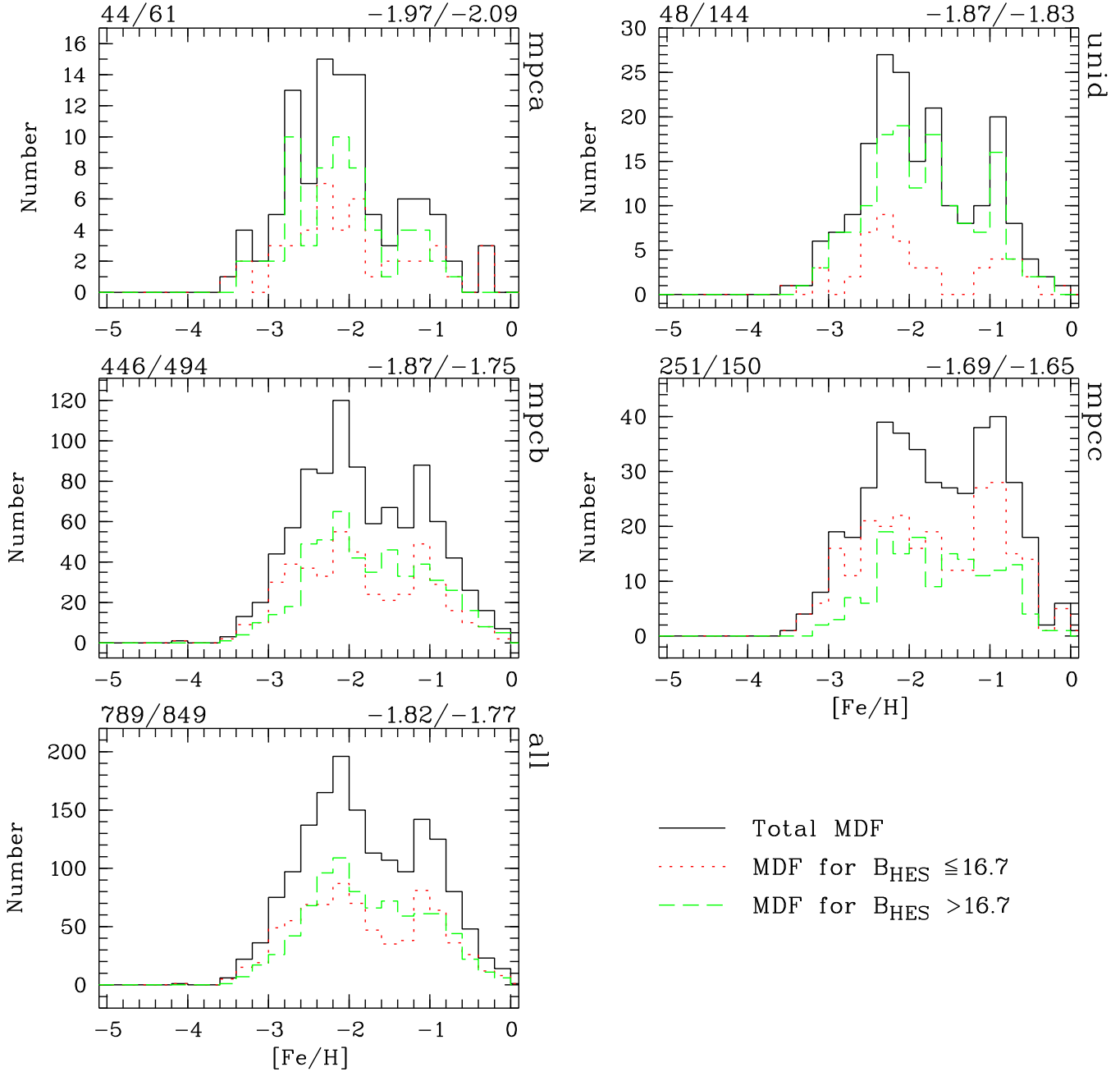


**Fig. 6.** Comparison of the MDFs of the bright ( $B \leq 16.7$  mag) and faint ( $B > 16.7$  mag) subsamples for each of the four candidate classes (upper four panels) as well as for the combined candidate sample (lower left panel). At the top left of each panel, the number of candidates belonging to the bright and faint sample, respectively, is listed; at the top right, the mean  $[\text{Fe}/\text{H}]$  of the samples is given. Faint candidates are over-represented in the class *unid*, because the visual classification for fainter candidates, which have lower quality HES spectra, was more difficult.

**Table 3.** The MDF of the Galactic halo field stars as constructed from the sample of 1638 HES with available spectroscopic follow-up observations by means of scaling to the full candidate sample of 3439 stars (for details see text). Note that for a proper comparison with the MDFs predicted by theoretical models, or the MDFs of other stellar populations, the selection efficiency of the HES as a function of  $[\text{Fe}/\text{H}]$  and  $(B - V)_0$  must be taken into account (see Tab. 4).

$[\text{Fe}/\text{H}]$	-4.50	-4.30	-4.10	-3.90	-3.70	-3.50	-3.30	-3.10	-2.90	-2.70	-2.50	-2.30	-2.10
$N$	0	0	2	0	0	12	45	73	160	198	281	337	399
$[\text{Fe}/\text{H}]$	-1.90	-1.70	-1.50	-1.30	-1.10	-0.90	-0.70	-0.50	-0.30	-0.10	+0.10	+0.30	+0.50
$N$	313	231	229	209	308	268	178	109	45	33	3	6	0

of the MDF at  $[\text{Fe}/\text{H}] < -4.0$  it is required to compile even larger statistically complete samples of metal-poor stars.

## 5. Comparison between theoretical MDFs and the halo MDF

In a comparison of the observed MDF with MDFs predicted by theoretical models, one has to take into account the modification of the shape of the MDF by the selection of metal-poor candidates employed in the HES. In particular, uncertainties  $\sigma_{\text{KP}}$  and  $\sigma_{B-V}$  of the measurements of the KP index and  $B-V$  in the HES spectra result in a scatter of stars with  $[\text{Fe}/\text{H}] > -2.5$  into the sample, and stars with  $[\text{Fe}/\text{H}] < -2.5$  out of the sample. Each theoretical MDF under investigation is therefore converted into an MDF as it would be observed in the HES, by applying the metal-poor star selection criteria used in the HES.

**Table 4.** Selection function for HES metal-poor candidates in the colour range  $0.5 < (B - V)_0 < 1.0$ , as determined from simulations.

[Fe/H]	Selected fraction at $(B - V)_0$					
	0.5	0.6	0.7	0.8	0.9	1.0
-4.05	1.000	1.000	1.000	1.000	1.000	1.000
-3.95	0.958	1.000	1.000	1.000	1.000	1.000
-3.85	1.000	0.962	1.000	1.000	1.000	1.000
-3.75	0.961	1.000	1.000	1.000	1.000	1.000
-3.65	0.982	0.987	1.000	1.000	1.000	1.000
-3.55	0.954	0.991	1.000	1.000	1.000	1.000
-3.45	0.920	0.991	0.997	0.996	1.000	1.000
-3.35	0.924	0.979	0.993	0.996	0.997	1.000
-3.25	0.901	0.976	0.989	0.991	0.985	1.000
-3.15	0.861	0.950	0.984	0.974	0.981	0.997
-3.05	0.816	0.919	0.958	0.954	0.953	0.983
-2.95	0.744	0.869	0.928	0.908	0.900	0.949
-2.85	0.668	0.801	0.879	0.852	0.839	0.918
-2.75	0.563	0.700	0.812	0.768	0.743	0.822
-2.65	0.455	0.583	0.715	0.658	0.617	0.709
-2.55	0.340	0.457	0.592	0.537	0.488	0.573
-2.45	0.232	0.337	0.462	0.406	0.364	0.433
-2.35	0.140	0.234	0.331	0.297	0.264	0.318
-2.25	0.075	0.149	0.222	0.203	0.187	0.217
-2.15	0.034	0.088	0.136	0.130	0.127	0.152
-2.05	0.013	0.046	0.079	0.081	0.085	0.100
-1.95	0.004	0.021	0.043	0.048	0.058	0.070
-1.85	0.001	0.009	0.022	0.028	0.041	0.051
-1.75	0.000	0.003	0.011	0.017	0.028	0.036
-1.65	0.000	0.001	0.006	0.010	0.020	0.028
-1.55	0.000	0.000	0.003	0.006	0.015	0.021
-1.45	0.000	0.000	0.001	0.004	0.010	0.017
-1.35	0.000	0.000	0.001	0.003	0.007	0.014
-1.25	0.000	0.000	0.001	0.002	0.004	0.008
-1.15	0.000	0.000	0.000	0.001	0.002	0.008
-1.05	0.000	0.000	0.000	0.001	0.001	0.004
-0.95	0.000	0.000	0.000	0.000	0.000	0.000
-0.85	0.000	0.000	0.000	0.000	0.000	0.000

The first step in the conversion of a theoretical MDF is the simulation of a sample of stars with a distribution in  $[\text{Fe}/\text{H}]$  according to that of the theoretical MDF under investigation.

The  $[\text{Fe}/\text{H}]$  values are then converted into pairs of KP and  $(B - V)_0$  by inverting the calibrations of Beers et al. (1999). Then, a subsample was selected such that it follows the distribution in  $(B - V)_0$  of the HES sample (see Fig. 1). Taking into account the distribution in  $(B - V)_0$  is important because the shape of the selection function is determined by  $\sigma_{\text{KP}}$ ,  $\sigma_{B-V}$ , and the gradient of  $[\text{Fe}/\text{H}]$  in the KP versus  $(B - V)_0$  parameter space (see Fig. 4 of Paper IV); it varies with  $(B - V)_0$ , as can be seen in Fig. 10.

The next step in the procedure was to add random Gaussian errors with standard deviations according to the known measurement uncertainties  $\sigma_{\text{KP}}$ ,  $\sigma_{B-V}$  in the HES to KP and  $(B - V)_0$  assigned to each star. Finally, the KP/ $(B - V)_0$  selection criterion was applied to the simulated sample of stars. The  $[\text{Fe}/\text{H}]$  distribution of the selected stars is the MDF as it would be observed in the HES.

We first consider the MDF predicted by the Simple Model of Galactic chemical evolution (Searle & Sargent 1972; Hartwick 1976). That model assumes that a fiducial “closed box” of primordial gas is enriched by successive stellar generations. Further model assumptions are that (i) the gas is well-mixed at all times (i.e there is a unique age-metallicity relation for the stars formed from that gas) and (ii) the stellar initial mass function (IMF) does not change with time. Analytical solutions can only be obtained if it is assumed that the evolutionary timescales of the enriching stars are negligible (the so-called Instantaneous Recycling Approximation or IRA). Such solutions can be generically obtained in the case of a closed box, and in some particular cases of outflow (gas loss from the box) and infall (gas flows into the box). Since the IRA turns out to be a very good approximation for elements ejected by massive stars, those analytical solutions can provide a powerful tool for the study of Galactic systems.

In the framework of the Simple Model, the shape of the MDF can be described in terms of a unique parameter, the “yield”, which is the ratio of the mass of newly-created metals to the mass locked in long-lived stars and stellar remnants. This is a very useful parametrization, because it is independent of the star formation history of the system (the major unknown in Galactic evolution studies). In the closed box model the yield depends only on the IMF (referred to as the “true yield”), while in the case of gaseous flows (infall and outflow) it depends also on their magnitude; this “effective yield”,  $y_{\text{eff}}$ , is always smaller than the true yield. It turns out that the MDF peaks at a metallicity equal to the effective yield; this simple result allows one to determine the effective yield and to constrain the underlying physics (IMF, outflow rate, etc.)

In Fig. 11, we compare the MDF of a Simple Model with  $y_{\text{eff}} = -1.7$  with the MDF observed in the HES. The HES MDF shows an excess of stars in the range  $-3.5 < [\text{Fe}/\text{H}] < -3.0$ . Alternatively, if the MDF of the Simple Model would be scaled such that it matches the observed MDF in this range, a large deficit of the number of observed stars in the range  $-3.0 < [\text{Fe}/\text{H}] < -2.0$  with respect to the Simple Model would result. It is also neither possible to reproduce with the Simple Model the sharp drop of the observed MDF at  $[\text{Fe}/\text{H}] = -3.6$ , nor the tail at  $[\text{Fe}/\text{H}] < -3.6$ .

Prantzos (2003) developed a modification of Simple Model, which includes early infall, and later outflow of gas; the IRA is

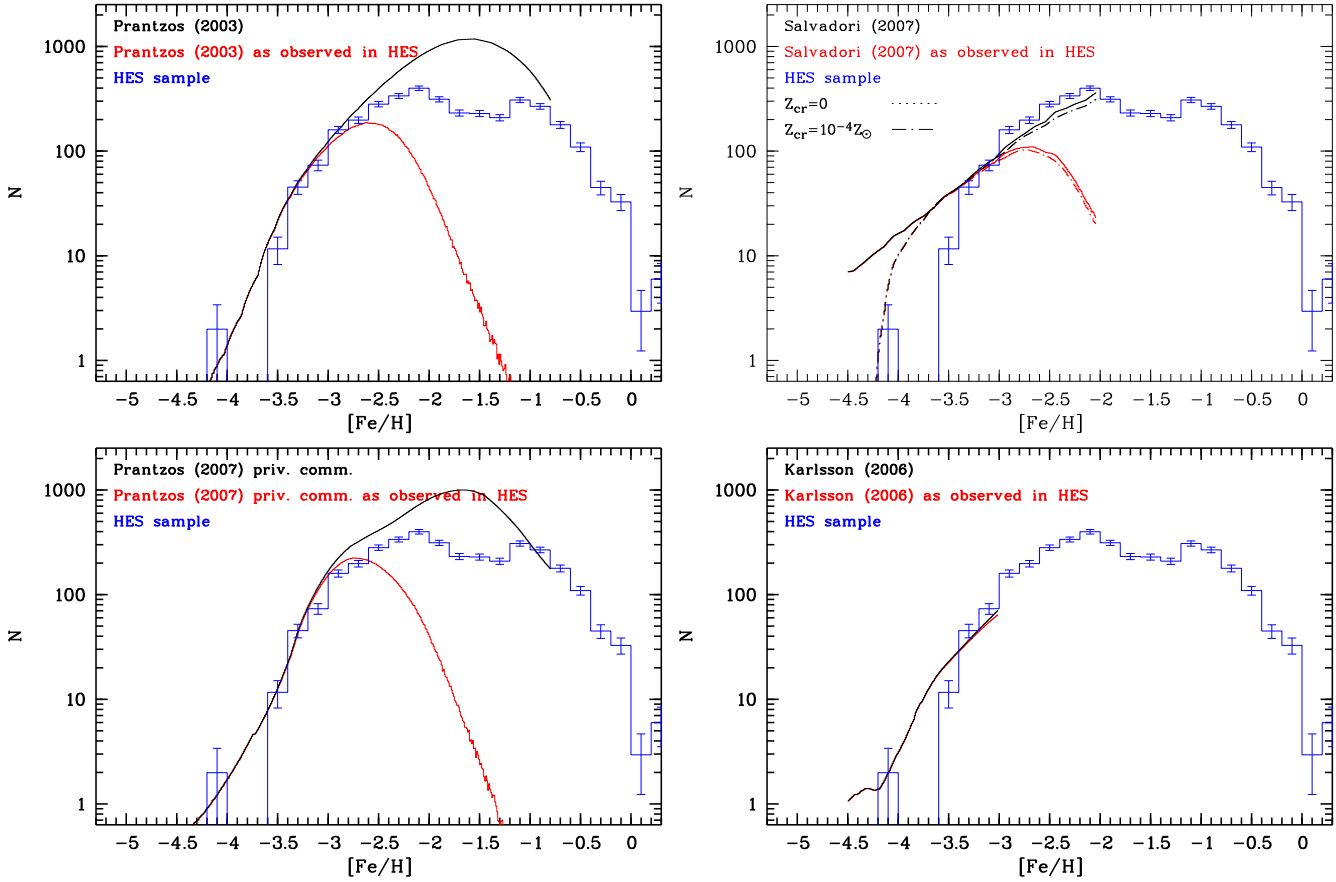


**Fig. 12.** Comparison of the MDF observed in the HES with theoretical predictions. Upper left panel: Prantzos (2003); upper right panel: Salvadori et al. (2007); lower left panel: Prantzos (2007); lower right panel: Karlsson (2006).

also relaxed in his model. His theoretical MDF matches the HES MDF well in the range  $-3.5 < [\text{Fe}/\text{H}] < -2.5$  (see Fig. 12), but neither the sharp drop at  $[\text{Fe}/\text{H}] \sim -3.6$  nor the tail at  $[\text{Fe}/\text{H}] < -3.6$  are predicted.

Two different approaches to modeling Galactic chemical evolution in the context of hierarchical structure formation can be found in the recent literature: (a) numerical simulations of the merger history of the Galaxy (e.g., Tumlinson 2006; Salvadori et al. 2007); (b) the semi-analytical approach suggested by Prantzos (2007). In Fig. 12, we compare MDFs predicted by the model of Salvadori et al. (2007) with that observed in the HES. A free parameter in this model is the critical metallicity for low-mass star formation,  $Z_{\text{cr}}$ . A model with  $Z_{\text{cr}} = 10^{-3.4} Z_{\odot}$  could probably reproduce the drop of the observed MDF at  $[\text{Fe}/\text{H}] \sim -3.6$ , but the tail at  $[\text{Fe}/\text{H}] < -4.0$  is not predicted.

Prantzos (2007) suggested that since the halo of the Galaxy has been assembled by merging of a large number of fragments, the MDF of the Galactic halo can be seen as the sum of the MDFs of these fragments. In his model, the chemical evolution histories of each of the fragments are still described by the Simple Model, using the observed mass-metallicity relation of dwarf galaxies to derive individual effective yields. The halo MDF is then produced by integrating over a mass function of the fragments determined in numerical simulations. The result is shown in Fig. 12. As for Prantzos (2003), the theoret-

ical MDF matches the HES MDF well in the range  $-3.5 < [\text{Fe}/\text{H}] < -2.5$ , but neither the sharp drop at  $[\text{Fe}/\text{H}] \sim -3.6$  nor the tail at  $[\text{Fe}/\text{H}] < -3.6$  are predicted.

Finally, we compare in Fig. 12 the HES MDF with that predicted by the stochastic chemical enrichment model of Karlsson (2006). While the model correctly predicts a tail  $[\text{Fe}/\text{H}] < -4.0$ , the drop of the observed MDF at  $[\text{Fe}/\text{H}] \sim -3.6$  is not present in the theoretical MDF.

## 6. Comparison of the halo field star MDF with that of other stellar populations

We have derived the MDF for field stars in the Galactic halo using the abundance distribution inferred from a sample of 1638 metal-poor stars selected from the HES. It is of great interest to compare this with the MDF found for other stellar populations, in particular for the system of Galactic globular clusters (hereafter GCs) and for the stars in dwarf spheroidal (dSph) galaxies. Since the most metal-poor Galactic GC has  $[\text{Fe}/\text{H}] \sim -2.5$ , we need to establish whether or not there is a real deficit of GCs at lower Fe-metallicities compared to the halo field.

For a proper comparison of the HES MDF with that of other stellar populations, it is mandatory that the selection function of the HES, as listed in Tab. 4, be taken into account. The values in that table can be used to correct the observed MDF for the selection of metal-poor candidates employed in the HES.

This is particularly important at  $[\text{Fe}/\text{H}] > -2.5$ , where the corrections are large, because typically less than half of the stars are actually picked up by the HES. Note that this incompleteness is intended, because the main aim of the search for metal-poor stars with the HES is to identify stars with  $[\text{Fe}/\text{H}] < -3.0$ . Therefore, the selection of candidate metal-poor stars was designed such that as many stars at  $[\text{Fe}/\text{H}] > -3.0$  as possible are rejected, while maintaining a high degree of completeness at  $[\text{Fe}/\text{H}] < -3.0$  (see Christlieb et al. 2008b for details).

For a star of a given  $[\text{Fe}/\text{H}]$ , the corrections are also a function of  $B - V$  color, being higher (more likely for a star to be included in the HES) for redder stars. The variation over the  $B - V$  color range of the HES sample can, in extreme cases at the higher metallicities, correspond to a variation of a factor of 8 in selection efficiency (see, e.g., the line for  $[\text{Fe}/\text{H}] = -1.95$  in Tab. 4).

For our comparison with the MDF of the Galactic GCs we adopt the  $[\text{Fe}/\text{H}]$  values from the current version of the online database of Harris (1996). The values for M15 and for NGC 7099 were updated with small corrections based on detailed abundance analyses carried out by J. Cohen and collaborators (Cohen & Huang 2008, in preparation; Cohen, Melendez & Huang 2008, in preparation). The HES is (intentionally) incomplete for  $[\text{Fe}/\text{H}] > -2.0$ , so we only consider the set of GCs with  $[\text{Fe}/\text{H}] < -1.95$ , which contains only 16 clusters. We note that many analyses have shown that the Galactic GCs exhibit the same behaviour of abundance ratios (such as the increase of  $[\text{Ca}/\text{Fe}]$  with decreasing  $[\text{Fe}/\text{H}]$ ) as the halo stars (e.g., Fig. 23 of Cohen et al. 2004) as do the halo stars. Thus, the conversion between a Ca line index and  $[\text{Fe}/\text{H}]$  adopted by the HES should be that one appropriate to halo field stars.

The comparison is shown in Fig. 13, where cumulative MDFs are shown for the HES sample and for the Galactic GC system. This figure clearly demonstrates that the Fe-metallicity distribution of the Galactic GCs does not match the cumulative MDF constructed from the observed, “raw” counts of stars given in Tab. 3. The solid, middle line in Fig. 13 corresponds to the case where corrections according to the dereddened  $B - V$  color of each individual star of the HES sample have been applied. Since these corrections are themselves uncertain, two other variants are shown in this figure and listed in Tab. 5 to indicate the potential impact of the choice of  $B - V$  color on the corrections. The first adopts the corrections for the bluest  $B - V$  color of Tab. 4, which are always the smallest, while the second uses that of the reddest  $B - V$  color of Tab. 4, which are always the largest.

Fig. 13 shows that once the selection efficiency corrections given Tab. 4 are applied, the halo field star MDF we deduce here is a good match to that of the Galactic GCs. Instead of expecting roughly 10% of the sample covering the range  $[\text{Fe}/\text{H}] < -1.95$  to have  $[\text{Fe}/\text{H}] < -3.0$ , we expect only  $\sim 2\%$  to be this metal deficient, when the selection efficiency for the HES is taken into account. At  $[\text{Fe}/\text{H}] < -2.5$ , the expected fraction decreases from 50% to 8%. Thus, the absence of any GC more metal-poor than  $-2.5$  dex among a sample of 16 clusters at  $[\text{Fe}/\text{H}] < -1.95$  is not surprising.

A similar situation holds for the stellar population in the dSph satellites of the Galaxy. It has been widely claimed (see,

**Table 5.** Cumulative halo MDF for  $[\text{Fe}/\text{H}] < -2.0$  as observed in the HES (column “Raw”), and corrected for the selection efficiency of the survey (columns 3–5). For details see text.

[Fe/H]	Raw	$(B - V)_0$ adopted for correction		
		Star	0.5	1.0
-4.30	0.0000	0.0000	0.0000	0.0000
-4.25	0.0013	0.0001	0.0003	0.0001
-4.20	0.0013	0.0001	0.0003	0.0001
-4.15	0.0013	0.0001	0.0003	0.0001
-4.10	0.0013	0.0001	0.0003	0.0001
-4.05	0.0013	0.0001	0.0003	0.0001
-4.00	0.0013	0.0001	0.0003	0.0001
-3.95	0.0013	0.0001	0.0003	0.0001
-3.90	0.0013	0.0001	0.0003	0.0001
-3.85	0.0013	0.0001	0.0003	0.0001
-3.80	0.0013	0.0001	0.0003	0.0001
-3.75	0.0013	0.0001	0.0003	0.0001
-3.70	0.0013	0.0001	0.0003	0.0001
-3.65	0.0013	0.0001	0.0003	0.0001
-3.60	0.0013	0.0001	0.0003	0.0001
-3.55	0.0039	0.0003	0.0009	0.0002
-3.50	0.0039	0.0003	0.0009	0.0002
-3.45	0.0103	0.0007	0.0024	0.0004
-3.40	0.0116	0.0008	0.0027	0.0005
-3.35	0.0141	0.0010	0.0033	0.0006
-3.30	0.0180	0.0013	0.0041	0.0008
-3.25	0.0282	0.0020	0.0065	0.0013
-3.20	0.0385	0.0028	0.0088	0.0018
-3.15	0.0488	0.0035	0.0112	0.0023
-3.10	0.0603	0.0044	0.0138	0.0029
-3.05	0.0770	0.0057	0.0177	0.0037
-3.00	0.0847	0.0063	0.0195	0.0041
-2.95	0.1065	0.0080	0.0246	0.0054
-2.90	0.1245	0.0096	0.0290	0.0064
-2.85	0.1502	0.0118	0.0353	0.0080
-2.80	0.1797	0.0148	0.0428	0.0100
-2.75	0.2131	0.0180	0.0517	0.0124
-2.70	0.2478	0.0220	0.0618	0.0153
-2.65	0.2555	0.0230	0.0642	0.0159
-2.60	0.3030	0.0293	0.0797	0.0205
-2.55	0.3273	0.0331	0.0888	0.0234
-2.50	0.3582	0.0388	0.1017	0.0275
-2.45	0.4031	0.0487	0.1234	0.0349
-2.40	0.4801	0.0691	0.1668	0.0508
-2.35	0.5225	0.0839	0.1953	0.0625
-2.30	0.5687	0.1019	0.2317	0.0790
-2.25	0.6226	0.1328	0.2810	0.1036
-2.20	0.6855	0.1812	0.3517	0.1448
-2.15	0.7664	0.2840	0.4627	0.2274
-2.10	0.8113	0.3679	0.5369	0.2997
-2.05	0.8858	0.5406	0.6848	0.4878
-2.00	0.9307	0.6959	0.7947	0.6458
-1.95	1.0000	1.0000	1.0000	1.0000

e.g. the review by Geisler et al. 2007) that these dSph stellar populations show a significant lack of stars with Fe-metallicity at  $[\text{Fe}/\text{H}] < -3.0$ . For example, Helmi et al. (2006) make this claim for the four systems for which they assembled the necessary data; i.e., Carina, Fornax, Sculptor and Sextans.

Abundances are now available for large samples of stars in the nearest dSph galaxies. We concentrate here on those where there is little or no evidence for recent star formation and for which suitable samples are available; specifically Draco, Ursa Minor, and Fornax. There are, however, two issues that arise in a comparison of the stellar population of the dSph galaxies with the Galactic halo MDF. The first is that these metallicities are derived from line indices which measure the strength of the Ca infrared triplet (CaT) in moderate-resolution spectra. The conversion from a Ca abundance to a Fe abundance is a crucial issue, since the dSph stellar population clearly shows a different trend of  $[\text{Ca}/\text{Fe}]$  versus  $[\text{Fe}/\text{H}]$  than does the Galactic halo (see, e.g., Geisler et al. 2005 or Monaco et al. 2007), with  $[\text{Ca}/\text{Fe}]$  being smaller at a given Fe-metallicity in dSph galaxies as compared to GCs and the halo field. The second is how the sample to be observed spectroscopically in the dSph is selected. If, e.g., an equal number of stars in each color bin is chosen to probe the full range of color across the upper RGB in a dSph, the sample may be biased in metallicity, because the position of the upper RGB in the color-magnitude diagram depends on  $[\text{Fe}/\text{H}]$ . Instead, a representative subset of stars reflecting the color distribution of the stars on the RGB should be chosen.

Bearing these caveats in mind, we have constructed the cumulative MDF for Draco, Ursa Minor, and Fornax. For Fornax, we use the VLT/FLAMES+GIRAFFE survey of Battaglia et al. (2006) (their Tab. 4) with measurements of the strength of the infrared Ca triplet. These were converted into Fe-metallicities using the relation established by Rutledge et al. (1997), which was calibrated using globular cluster giants. Their sample includes 48 stars with  $[\text{Fe}/\text{H}] < -1.9$ . Battaglia advises (priv. comm.) that their sample should be unbiased with respect to metallicity. Battaglia et al. (2008) discussed the accuracy of their conversion between Ca triplet line strength and  $[\text{Fe}/\text{H}]$ , given the difference in the behavior of  $[\text{Ca}/\text{Fe}]$  with Fe-metallicity between GCs and dSph populations. Using a comparison of high dispersion abundance analyses with their results from CaT measurements for a limited sample of dSph giants, they conclude that their Fe-metallicities are robust to within  $\pm 0.2$  dex, but they use a slightly modified CaT to Fe transformation in this later paper. In any case, the left panel of Fig. 14 shows that the Fornax dSph is deficient in stars with  $[\text{Fe}/\text{H}] < -2.0$  relative to the MDF of the halo field stars only when the HES raw counts are used. Once the selection efficiencies are folded in, the Fornax cumulative MDF at  $[\text{Fe}/\text{H}] < -2.0$  is consistent with that of the Galactic halo field stars as inferred from the HES, just as we found above for the Galactic GCs.

We carry out the same comparison for Draco and for Ursa Minor using the database of Winnick (2003). She measured CaT line strengths from spectra obtained with the multi-fiber instrument Hydra at the WIYN telescope. Her sample is selected from radial velocity members with no metallicity bias. Winnick calibrates a relation between both  $[\text{Ca}/\text{H}]$  and  $[\text{Fe}/\text{H}]$  and CaT from observations of GC giants, making no attempt to take into account the difference in the behavior of  $[\text{Ca}/\text{Fe}]$  with  $[\text{Fe}/\text{H}]$  in these two stellar populations. We therefore apply a correction of  $+0.35$  dex to her tabulated  $[\text{Fe}/\text{H}]$  values to put them onto the GC Fe-metallicity scale. The case of Draco, with

74 stars at  $[\text{Fe}/\text{H}] < -1.9$  (40 of which have  $[\text{Ca}/\text{H}] < -1.9$ ) is shown in the lower panels of Fig. 14. The  $[\text{Ca}/\text{H}]$  MDF she infers from her CaT line strengths is consistent, to within the uncertainties, with the halo Fe-MDF, once the selection efficiency of the HES is taken into consideration, as is the case for UMi. The MDF for  $[\text{Fe}/\text{H}]$  in Draco is consistent as well, given the uncertainties in the conversion from CaT measurements to  $[\text{Fe}/\text{H}]$ .

We thus find that the MDF of the Galactic halo field stars as derived from the HES is statistically indistinguishable from that of the Galactic globular cluster system and of the stellar population of the nearest dSph satellites of the Galaxy, contrary to the result of Helmi et al. (2006). This holds over the range  $[\text{Fe}/\text{H}] < -1.9$  after the selection efficiency corrections to the apparent MDF from the HES have been applied.

Recently, Kirby et al. (2008) found 15 stars with  $[\text{Fe}/\text{H}] < -3.0$  in seven of the ultra-faint dSph galaxies recently discovered by the SDSS. Since all these very low luminosity galaxies have mean  $[\text{Fe}/\text{H}]$  values of  $-1.9$  dex or lower, this is perhaps not surprising. While the validity of the calibration of the CaT with metallicity is debatable at very low metallicity (see, e.g., Starkenburg 2009), Kirby et al. (2008) developed a spectral synthesis technique which does not use the CaT at all. Cohen & Huang (2008, in preparation) have obtained high resolution spectra of a sample of stars in the Draco dSph, one of the more luminous of the dSph satellites of the Galaxy, and found one star with  $[\text{Fe}/\text{H}] < -3.0$  in that dSph as well. Thus, extremely metal-poor stars are present, albeit in small numbers, in both the ultra-faint and classical dSph satellites of the Galaxy.

## 7. Discussion and conclusions

In Sect. 5 we have shown that a reasonable agreement with the overall shape of the HES MDF can be obtained for  $[\text{Fe}/\text{H}] > -3.6$  by most models of Galactic chemical evolution, but none of them predict the sharp drop at  $[\text{Fe}/\text{H}] \sim -3.6$  seen in the HES MDF. The lack of stars at  $[\text{Fe}/\text{H}] < -3.6$  is highly significant: The models typically predict that about ten such stars should be present in the HES sample, while only two are found. It remains to be investigated whether the drop can be reproduced by modifying some of the assumptions of the models, or by adding further ingredients.

To our knowledge, the stochastic chemical enrichment model of Karlsson (2006) is the only model which predicts a very sparse tail of stars at  $[\text{Fe}/\text{H}] < -4.0$ , in agreement with the halo MDF observed in the HES.

In the  $\Lambda$ CDM picture, the Galactic halo was largely built out of disrupted satellite galaxies. If stars had already formed within them at the time of accretion, then the MDF of the Galactic halo and of the existing dSph galaxies should agree at the metal-poor end with regard to the presence of a weak tail of stars with  $[\text{Fe}/\text{H}] < -3.0$ . It is thus reassuring for the  $\Lambda$ CDM scenario that our analysis shows that the dSph galaxies do not appear to be deficient in extremely metal-poor stars, in contrast to the claims of e.g. Helmi et al. (2006). An important question remaining to be answered is how the abundance ratios

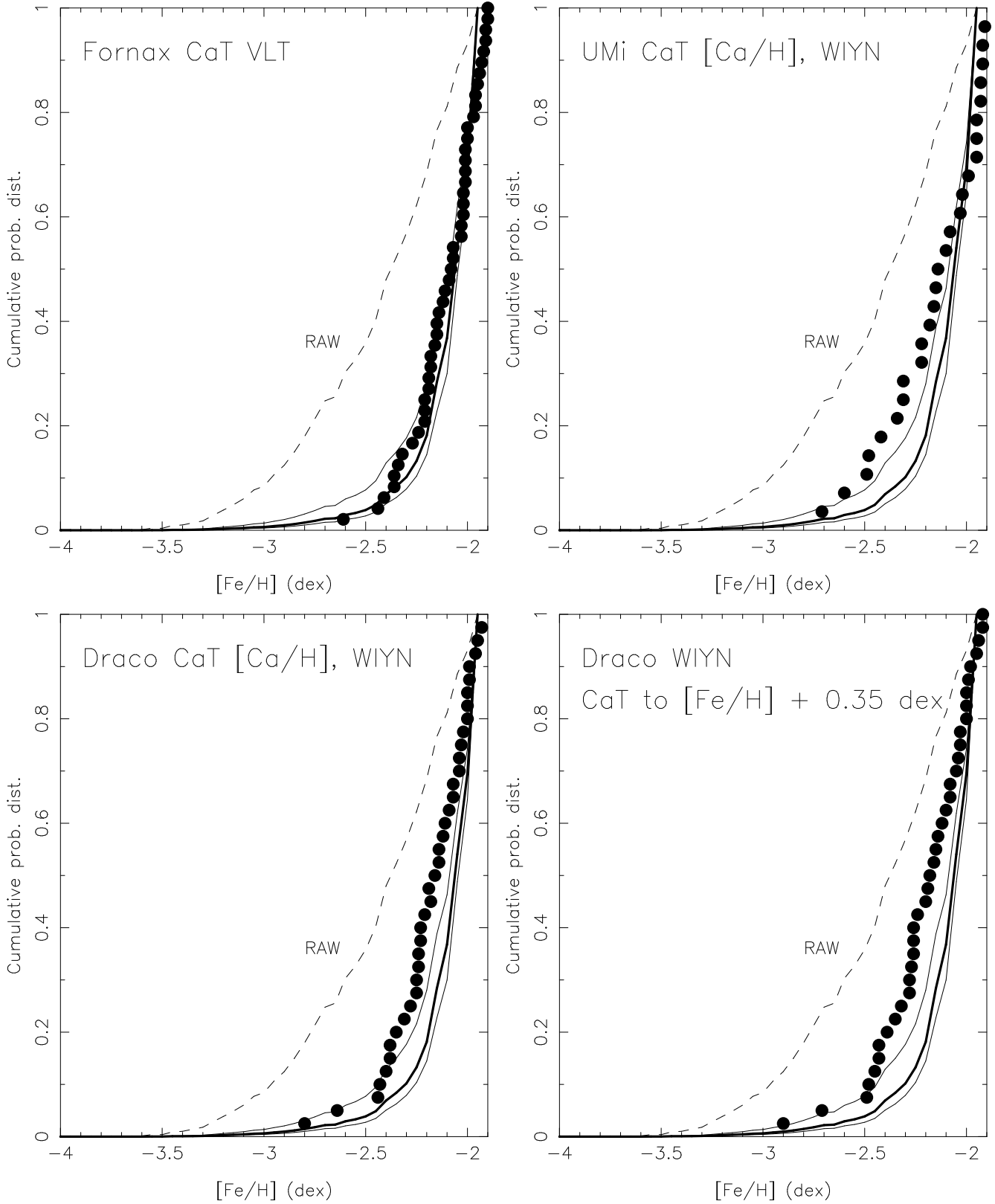


**Fig. 14.** Cumulative MDF for  $[\text{Fe}/\text{H}] < -2.0$  as observed in the HES (dashed line), and with corrections for the HES selection efficiency applied (solid lines; see the caption of Fig. 13 and the text for a detailed explanation). The filled circles indicate the cumulative MDFs of Fornax (upper left panel), Ursa Minor (upper right panel), Draco, using  $[\text{Ca}/\text{H}]$  (lower left panel), and Draco, using a conversion of  $[\text{Ca}/\text{H}]$  to  $[\text{Fe}/\text{H}] + 0.35$  dex (lower right panel).

of the dSph stars at  $[\text{Fe}/\text{H}] < -3.0$  compare with those of the Galactic halo stars.

Since the HES and the HK survey are in-situ surveys that predominantly sample the inner-halo population of the Galaxy (with  $R < 15$  kpc), it is mandatory to consider the possibility that the (for now, poorly studied) outer-halo population of the Galaxy may indeed contain significant numbers of stars with  $[\text{Fe}/\text{H}] < -3.6$ , as might be indicated by the shift of the peak metallicity of the other-halo stars studied by Carollo et al. (2007) to  $[\text{Fe}/\text{H}] = -2.2$ , a factor of three lower than the peak metallicity of inner-halo stars. This possibility is being actively pursued by high-resolution spectroscopic follow-up of stars that are likely to be members of the outer-halo population, based on their local kinematics, by a number of groups.

*Acknowledgements.* We thank T. Karlsson, N. Prantzos, and S. Salvadori for providing us with electronic versions of published theoretical MDFs, and for enlightening discussions. We are grateful to S. Ryan for valuable comments on an earlier version of this paper. N.C. and D.R. acknowledge financial support from Deutsche Forschungsgemeinschaft through grants Ch 214/3 and Re 353/44. N.C. is also supported by the Knut and Alice Wallenberg Foundation. J.G.C. is grateful to NSF grant AST-0507219 for partial support. T.C.B. acknowledges partial funding for this work from grants AST 04-06784, AST 06-07154, AST 07-07776, and PHY 02-16873: Physics Frontier Center/Joint Institute for Nuclear Astrophysics (JINA), all awarded by the US National Science Foundation. M.S.B. and J.E.N. acknowledge support from the Australian Research Council under grants DP0342613 and DP0663562. A.F. acknowledges support from the W.J. McDonald Fellowship of the McDonald Observatory. P.S.B. is a Royal Swedish Academy of Sciences Research Fellow supported by a grant from the Knut and Alice Wallenberg Foundation. P.S.B. also acknowledges the support of the Swedish Research Council.

## References

- Aoki, W., Frebel, A., Christlieb, N., et al. 2006, *ApJ*, 639, 897, astro-ph/0509206
- Barklem, P., Christlieb, N., Beers, T., et al. 2005, *A&A*, 439, 129, astro-ph/0505050
- Battaglia, G., Helmi, A., Tolstoy, E., et al. 2008, *ApJ*, 681, L13
- Battaglia, G., Tolstoy, E., Helmi, A., et al. 2006, *A&A*, 459, 423
- Beers, T. & Christlieb, N. 2005, *ARA&A*, 43, 531
- Beers, T., Preston, G., & Shectman, S. 1985, *AJ*, 90, 2089
- Beers, T. C. 1999, in *ASP Conf. Ser.*, Vol. 165, *The Third Stromlo Symposium: The Galactic Halo*, ed. B. Gibson, T. Axelrod, & M. Putman, 202–212
- Beers, T. C., Preston, G. W., & Shectman, S. A. 1992, *AJ*, 103, 1987
- Beers, T. C., Rossi, S., Norris, J. E., Ryan, S. G., & Shefler, T. 1999, *AJ*, 117, 981
- Bessell, M., Christlieb, N., & Gustafsson, B. 2004, *ApJ*, 612, L61
- Bond, H. E. 1981, *ApJ*, 248, 606
- Bromm, V., Ferrara, A., Coppi, P., & Larson, R. 2001, *MNRAS*, 328, 969
- Bromm, V. & Loeb, A. 2003, *Nature*, 425, 812
- Carney, B., Laird, J., Latham, D., & Aguilar, L. 1996, *AJ*, 112, 668
- Carollo, D., Beers, T., Chiba, M., et al. 2007, *Nature*, 450, 1020
- Cayrel, R., Depagne, E., Spite, M., et al. 2004, *A&A*, 416, 1117
- Christlieb, N., Bessell, M., Beers, T., et al. 2002, *Nature*, 419, 904
- Christlieb, N., Bessell, M., & Eriksson, K. 2008a, in preparation
- Christlieb, N., Green, P., Wisotzki, L., & Reimers, D. 2001a, *A&A*, 375, 366
- Christlieb, N., Gustafsson, B., Korn, A., et al. 2004, *ApJ*, 603, 708, astro-ph/0311173
- Christlieb, N., Schörck, T., Frebel, A., et al. 2008b, *A&A*, 484, 721
- Christlieb, N., Timothy C. Beers, Thom, C., et al. 2005, *A&A*, 431, 143
- Christlieb, N., Wisotzki, L., Reimers, D., et al. 2001b, *A&A*, 366, 898
- Cohen, J., Christlieb, N., McWilliam, A., et al. 2008, *ApJ*, 672, 320
- Cohen, J., Christlieb, N., McWilliam, A., et al. 2004, *ApJ*, 612, 1107
- Cohen, J., McWilliam, A., Shectman, S., et al. 2006, *AJ*, 132, 137
- Cohen, J., Shectman, S., Thompson, I., et al. 2005, *ApJ*, 633, L109
- Frebel, A., Aoki, W., Christlieb, N., et al. 2005, *Nature*, 434, 871
- Frebel, A., Christlieb, N., Norris, J., Aoki, W., & Asplund, M. 2006a, *ApJ*, 638, L17
- Frebel, A., Christlieb, N., Norris, J., et al. 2006b, *ApJ*, 652, 1585
- Frebel, A., Johnson, J., & Bromm, V. 2007, *MNRAS*, 380, L40
- Geisler, D., Smith, V. V., Wallerstein, G., Gonzalez, G., & Charbonnel, C. 2005, *AJ*, 129, 1428
- Geisler, D., Wallerstein, G., Smith, V. V., & Casetti-Dinescu, D. I. 2007, *PASP*, 119, 939
- Gunn, J. E., Carr, M., Rockosi, C., et al. 1998, *AJ*, 116, 3040
- Harris, W. E. 1996, *AJ*, 112, 1487
- Hartwick, F. 1976, *ApJ*, 209, 418
- Helmi, A., Irwin, M. J., Tolstoy, E., et al. 2006, *ApJ*, 651, L121
- Ivezic, Z., Sesar, B., Juric, M., et al. 2008, *ApJ*, in press
- Karlsson, T. 2006, *ApJ*, 641, L41
- Kim, Y., Demarque, P., Yi, S., & Alexander, D. 2002, *ApJS*, 143, 499
- Kirby, E., Simon, J., Geha, M., Guhathakurta, P., & Frebel, A. 2008, *ApJ*, in press
- Lee, Y., Beers, T., Sivarani, T., et al. 2008a, *AJ*, submitted
- Lee, Y., Beers, T., Sivarani, T., et al. 2008b, *AJ*, submitted
- Lucatello, S., Beers, T., Christlieb, N., et al. 2006, *ApJ*, 652, L37
- Monaco, L., Bellazzini, M., Bonifacio, P., et al. 2007, *A&A*, 464, 201
- Norris, J. 1999, in *ASP Conf. Ser.*, Vol. 165, *The Third Stromlo Symposium: The Galactic Halo*, ed. B. Gibson, T. Axelrod, & M. Putman, 213–224
- Norris, J., Christlieb, N., Korn, A., et al. 2007, *ApJ*, 670, 774
- Omukai, K. 2000, *ApJ*, 534, 809

- Prantzos, N. 2003, *A&A*, 404, 211
- Prantzos, N. 2007, in *EAS Publications Series*, Vol. 24, *Chemodynamics: from first stars to local galaxies*, ed. E. Emsellem, H. Wozniak, G. Massacrier, J.-F. Gonzalez, J. Devriendt, & N. Champavert, 3–14
- Prieto, C. A., Sivarani, T., Beers, T., et al. 2008, *AJ*, submitted
- Reimers, D. 1990, *The Messenger*, 60, 13
- Rutledge, G. A., Hesser, J. E., Stetson, P. B., et al. 1997, *PASP*, 109, 883
- Ryan, S. & Norris, J. 1991, *AJ*, 101, 1865
- Salvadori, S., Schneider, R., & Ferrara, A. 2007, *MNRAS*, 381, 647
- Schlegel, D., Finkbeiner, D., & Davis, M. 1998, *ApJ*, 500, 525
- Searle, L. & Sargent, W. 1972, *ApJ*, 173, 25
- Starkenbug, E. 2009, in *Chemical Evolution of Dwarf Galaxies and Stellar Clusters*, ed. F. Primas & A. Weiss, MPA/ESO/MPE/USM Garching Astronomy Conferences, MPA/ESO/MPE/USM (Garching: ESO)
- Tumlinson, J. 2006, *ApJ*, 641, 1
- Umeda, H. & Nomoto, K. 2003, *Nature*, 422, 871
- Winnick, R. A. 2003, PhD thesis, Yale University
- Wisotzki, L., Christlieb, N., Bade, N., et al. 2000, *A&A*, 358, 77
- Wisotzki, L., Köhler, T., Groote, D., & Reimers, D. 1996, *A&AS*, 115, 227
- York, D., Adelman, J., Anderson, J., & et al. 2000, *AJ*, 120, 1579

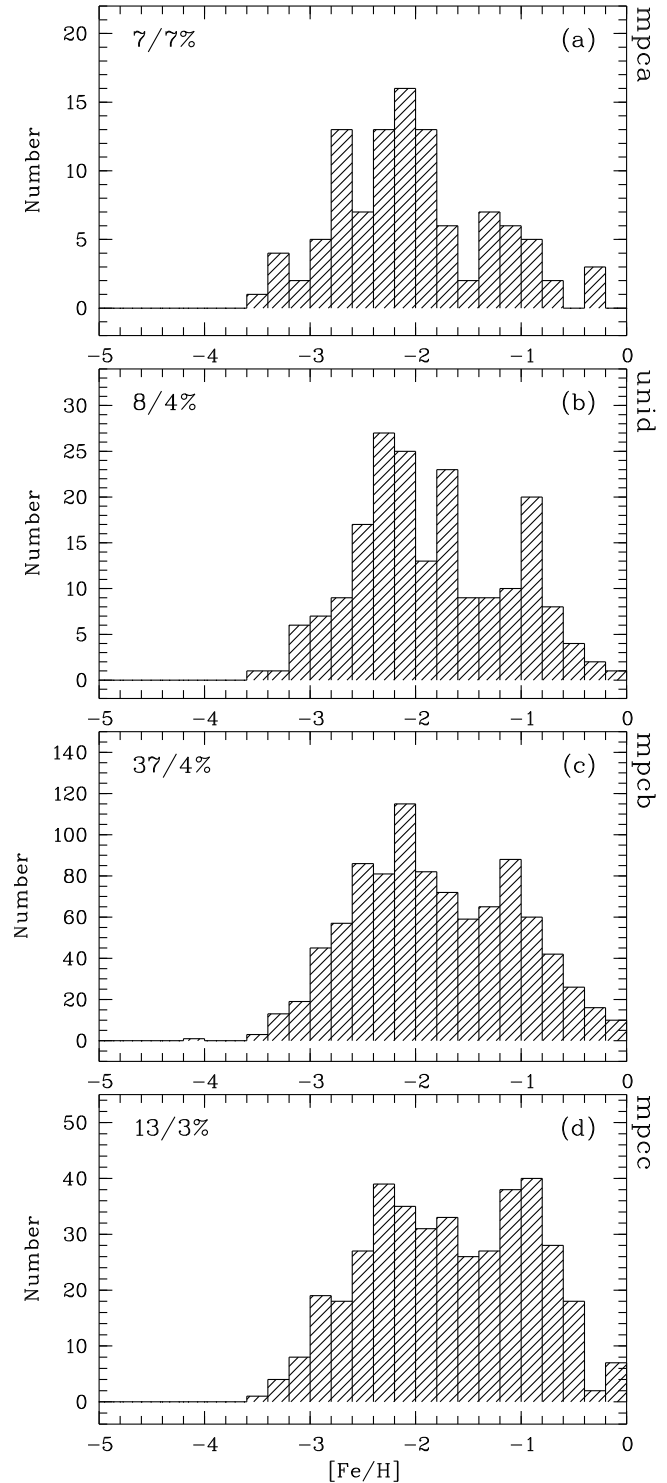


**Fig. 7.** Metallicity distribution of the HES sample of 1638 stars, divided by candidate class. In the upper left corner of each panel, the number of stars with  $[\text{Fe}/\text{H}] < -3.0$  and the percentage of such stars within each candidate class is indicated.

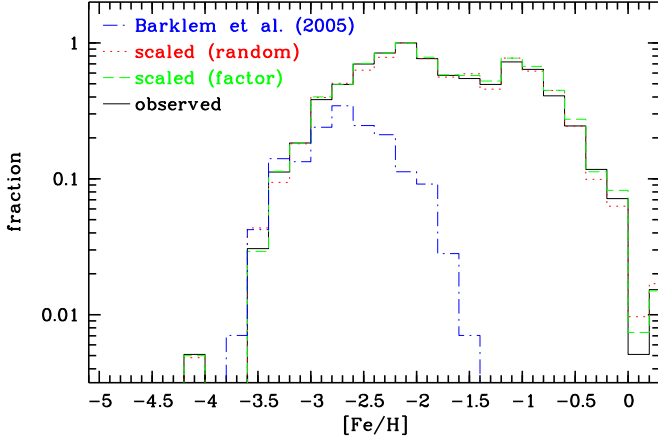


**Fig. 8.** Comparison of the MDF of the 1638 observed HES stars (solid black line) with the MDFs constructed by means of random scaling and co-addition of the class-wise MDFs (grey dashed line) and scaling by factors (grey dotted) line, and with the MDF of the HERES sample analysed by (Barklem et al. 2005, grey dash-dotted line). The latter sample is biased against stars of  $[\text{Fe}/\text{H}] > -3.0$ , because most stars at higher metallicity were intentionally removed due to the science aims of that survey.

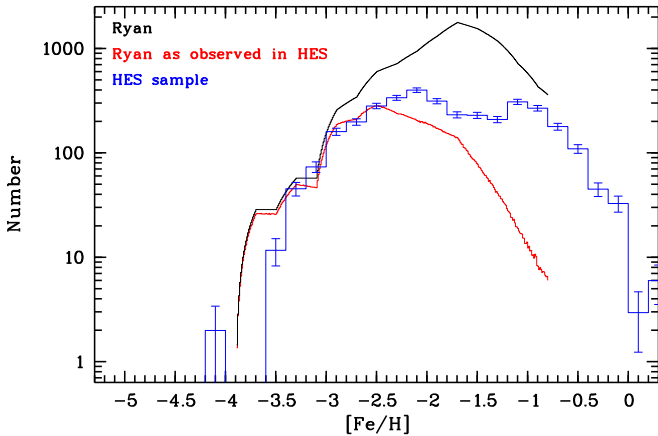


**Fig. 9.** Comparison of the halo MDF constructed from the HES sample (solid grey line with error bars) with that of Ryan & Norris (1991) scaled to match the HES MDF in the range  $-3.4 < [\text{Fe}/\text{H}] < -2.5$ .

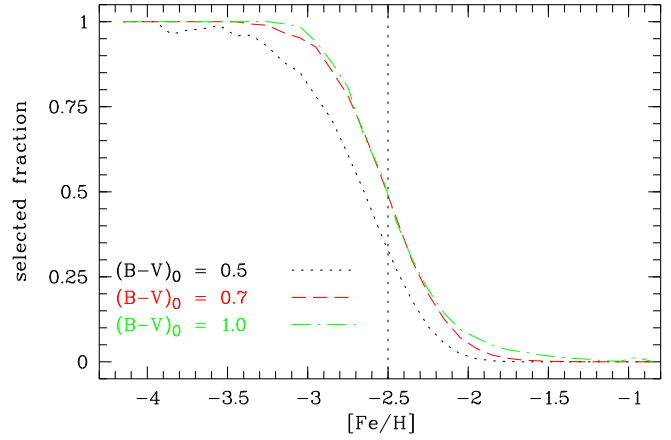


**Fig. 10.** Selection function for HES metal-poor candidates of  $(B-V)_0 = 0.5, 0.7,$  and  $1.0$ .

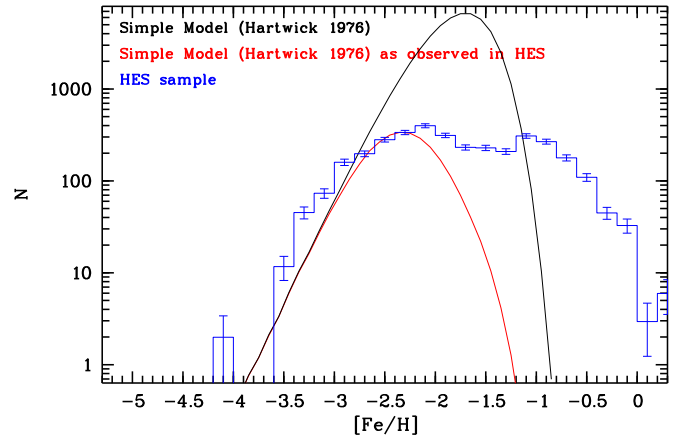


**Fig. 11.** Comparison of the MDF of a Simple Model with  $y_{\text{eff}} = -1.7$  with the MDF observed in the HES. For the comparison, only the metallicity range below  $[\text{Fe}/\text{H}] \sim -2.0$  should be taken into account, because at higher  $[\text{Fe}/\text{H}]$  the HES sample is contaminated with thick disk and thin disk stars.

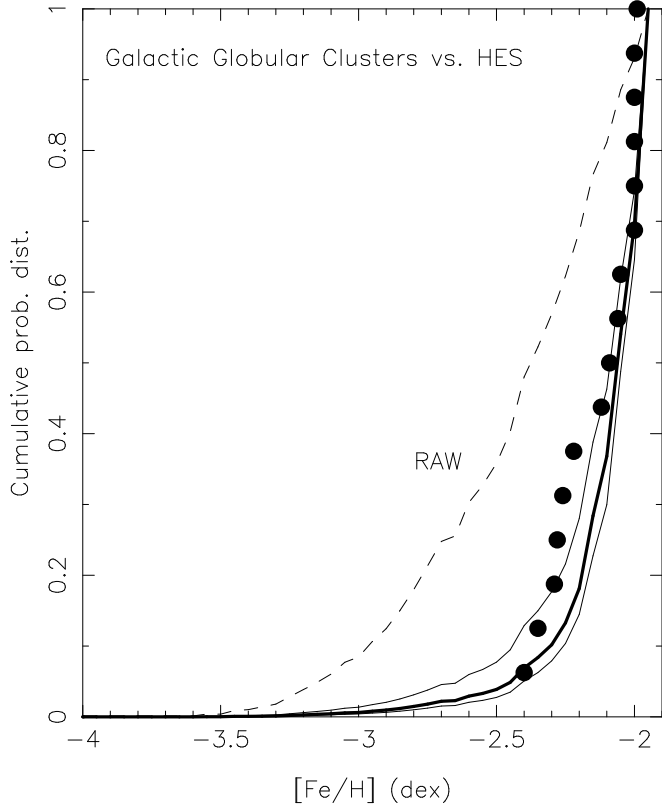


**Fig. 13.** Cumulative MDF for  $[\text{Fe}/\text{H}] < -2.0$  as observed in the HES (dashed line), and with corrections for the HES selection efficiency applied (solid lines). Three different ways of applying the corrections are shown to illustrate their uncertainty: Multiplication of the observed metal-poor star counts with the corrections for  $(B - V)_0 = 1.0$  (upper solid line), the  $(B - V)_0$  color appropriate for each individual star in the HES sample (thick, middle line), and the corrections for  $(B - V)_0 = 0.5$  (lower solid line). The cumulative MDF of the GCs  $[\text{Fe}/\text{H}] < -1.95$  is shown by filled circles. It agrees well with that of the halo field stars if the selection efficiency corrections are applied.